

Hexagonal Selenium Nanowires Synthesized via Vapor-Phase Growth

Lei Ren, Hongzhou Zhang, Pingheng Tan,[†] Yaofeng Chen, Zhensheng Zhang, Yongqin Chang, Jun Xu, Fuhua Yang,[†] and Dapeng Yu*

School of Physics, State Key Laboratory for Mesoscopic Physics, and Electron Microscopy Laboratory, Peking University, Beijing 100871, People's Republic of China, and National Laboratory for Superlattices and Microstructures, Institute of Semiconductors, Chinese Academy of Sciences, Beijing 100083, People's Republic of China

Received: July 29, 2003; In Final Form: January 15, 2004

Hexagonal Se nanowires were synthesized using a simple vapor-phase growth with the assistance of the silicon powder as a source material, which turned out to be very important in the growth of the Se nanowires. The morphology, microstructure, and chemical compositions of the nanowires were characterized using various means (XRD, SEM, TEM, XPS, and Raman spectroscopy). The possible growth mechanism of the Se nanowires was explained. The as-grown Se nanowires may find wide applications in biology and optoelectronics.

Introduction

Selenium is known as an essential element for life due to its great nutritional effect and many fascinating properties in biology and chemistry: for example, protecting cells against the effects of free radicals that are produced during normal oxygen metabolism, reinforcing the normal functions of the immune system and thyroid gland, localizing malfunction in the pancreas, and the safe uses of selenium in agriculture.¹ However, selenium attracts even more attention in the physical sciences than in the biosciences¹ because it exhibits many more promising physical properties, such as the anisotropy of the thermoconductivity, superconductivity of metallic selenium below 6.7 K,² a high photoconductivity ($8 \times 10^4 \text{ S cm}^{-1}$), hydration and oxidation catalytic activity, and high piezoelectric, thermoelectric, and nonlinear optical responses.³ It thus has been of tremendous importance in extensive applications, for example, electrophotographic materials,⁴ and Xerox copying machines and rectifiers.³ On the other hand, quasi-one-dimensional (1D) materials have attracted much attention for both their importance in mesoscopic physics and potential applications in fabricating novel nanoelectronic, optoelectronic, electrochemical, and electromechanical devices.^{5,6} Recently, selenium nanowires have been fabricated through a few approaches, e.g., laser ablation,⁷ reduction method,⁴ catalytic growth,⁸ and solution-phase approach.^{3,9} So far, most of the reported methods for Se nanowire growth are chemical routines. Compared with the above-mentioned methods, the physical evaporation approach remains a valuable technique for fabrication of low-dimensional materials because of its simplicity and low cost. Here we report a vapor-phase growth of hexagonal selenium nanowires by physical evaporation of selenium powder using silicon powders as catalyst.

Experimental Section

Our fabrication of Se nanowires was based on a thermal evaporation process of Se powder with Si powder as catalyst.

The synthesis apparatus has been described in our previous papers.¹⁰ The synthesis process was carried out in a tube furnace. The selenium powder ($\geq 99.95\%$) in a quartz crucible was placed in the front of the quartz tube. A long quartz plate covered with silicon powder (99%) was placed at the central zone of the quartz tube. During the experiment, a constant flow of argon gas (99.9%, 140 sccm) was introduced into the system. The system was evacuated by a mechanic pump, and the pressure inside the quartz tube was kept at 150 Torr. The temperature of the system was elevated to the reaction temperature. The temperature near the Se source and the Si-covered quartz plate was around 680 °C and 950 °C, respectively. The products were collected by a copper collector cooled by water (~ 100 °C). Therefore, a temperature gradient of about 20 °C/cm was established from the Si powders to the collector. The whole reaction lasted for 3 h. After cooling to room temperature, the collector was found covered with a brick-red layer, which was scratched off for investigation.

The morphology of the samples was analyzed by using a field emission Strata DB235 FIB working at scanning microscope mode (SEM) and a transmission electron microscope (TEM, Tecnai F30) equipped with energy dispersive spectroscopy (EDS). Raman scattering measurements were conducted to further analyze the structures of the products, while X-ray photoelectron spectroscopy (XPS) depicted the chemical compositions of the samples.

Results and Discussion

Figure 1a shows the XRD spectrum of the as-grown samples. The peak positions and their relative intensities are very consistent with a hexagonal selenium phase of with random crystallographic orientation. The lattice constants calculated from the diffraction patterns are $a = 0.437 \text{ nm}$, $c = 0.495 \text{ nm}$. This crystal structure with D_3^6 symmetry is a very stable crystalline form of selenium, which consists of parallel spiral chains of selenium atoms terminating at the corners and center of a regular hexagon. The bonding within the chains is much stronger than the bonding between the chains.^{2,3} The as-grown samples were then dispersed in alcohol solution by sonication and dripped onto silicon wafers and carbon-coated holey Cu grids destined

* Author to whom correspondence should be addressed. Tel: +86-010-62759474. Fax: +86-010-62759474. E-mail: yudp@pku.edu.cn.

[†] Institute of Semiconductors, Chinese Academy of Sciences.

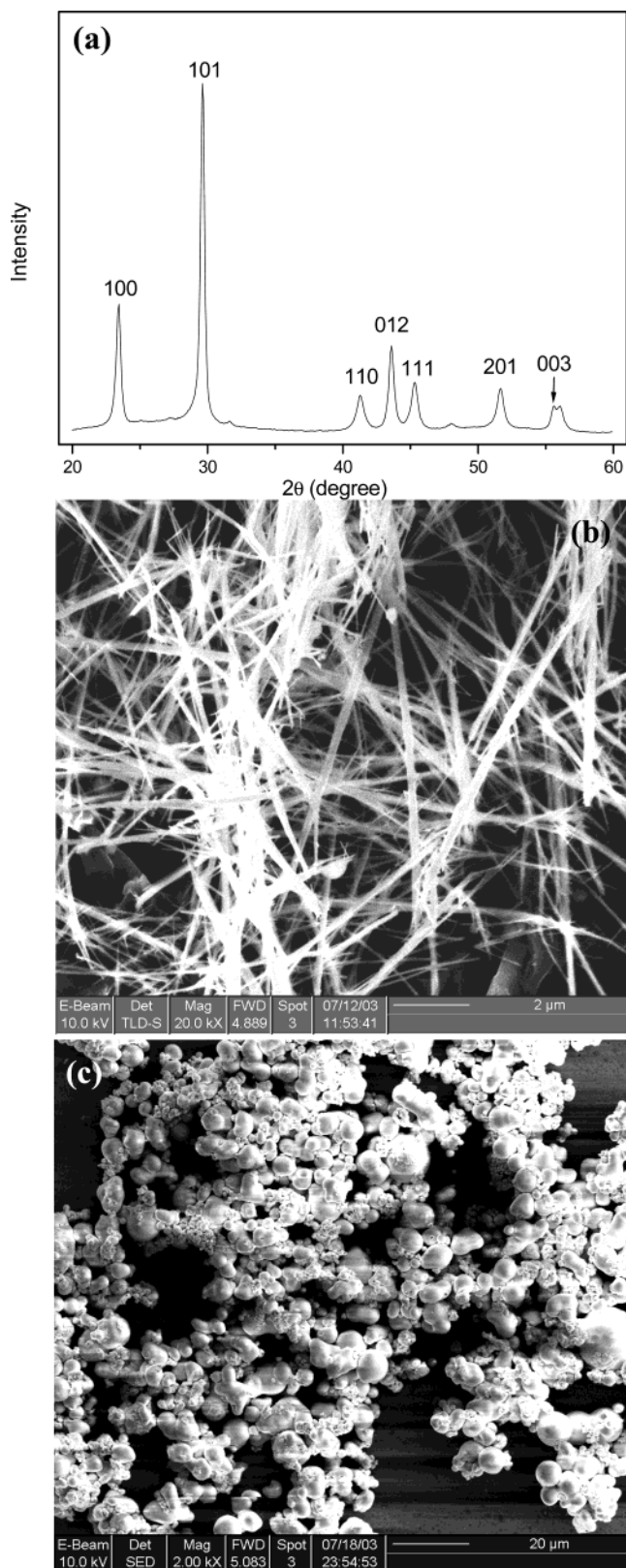


Figure 1. (a) XRD spectrum from bulk quantity of the products. The peak positions and relative intensities confirm that the products are of a hexagonal Se phase. (b) SEM image revealing the general morphology of the Se nanowires. (c) SEM image showing that only micro-sized bubbles are observed in case no silicon powder was added to the source materials.

for SEM and TEM investigations, respectively. The SEM image illustrated in Figure 1b reveals the general morphology of the Se nanowires grown with Si as a catalyst. It is seen that the Se

nanowires are over several micrometers in length and 50–100 nm in diameter. In contrast, only micro-sized bubbles are observed if no silicon powder was added to the source materials, as is shown in the SEM image in Figure 1c, which reveals the crucial role that silicon plays in the growth of the Se nanowires.

The microstructure of the as-grown samples is further analyzed using TEM and HRTEM. As shown in Figure 2a, the typical TEM image discloses the general morphology of the samples. The Se nanowires exhibit straight rod shapes. The length of the wires, as shown in Figure 2a, can be up to several micrometers. The finest nanowire is around 20 nm. The diameter of the Se nanowires is not uniform, varying in the range of 20–300 nm. One single nanowire is magnified in Figure 2b. The bright and dark strips on the nanowire reveal the single crystalline nature of the samples. The chemical composition corresponding to the single nanowire is investigated by EDS and depicted in Figure 2c. Only Se peaks are observed from the samples, confirming that the products are Se nanowires, while the C and Cu peaks originate from the supporting carbon membrane and copper grids, respectively. The HRTEM image in Figure 2d can give further insight into the details of the structure. The lattice fringes can be clearly distinguished. The spacing between two fringes is about 0.16 nm, which corresponds to the interplanar spacing of the (003) planes, that is parallel to the *c*-axis direction. The continuous fringes demonstrate that the Se nanowires have a low defect density. An amorphous layer with 2 nm in thickness is observed sheathing the Se nanowires, as is indicated with a black arrow. The fast Fourier transform (FFT) corresponding to the HRTEM image is shown as the inset of Figure 2d. The nanowires turned out to be very sensitive to longer time electron beam irradiation, in particular at high magnification.

To further clarify the chemical situations of the elements, we measured XPS of the samples, and the Se 3d peaks are shown in Figure 3a. There are two peaks positioned at 59.2 eV and 55.7 eV, which arise from Se–O and Se–Se bonds, respectively. The percentage of Se–O bonds is much lower than that of the Se–Se bonds, suggesting that a very small amount of Se is in the oxidized state. According to our HRTEM results (Figure 2d), the Se–O bonds are most likely from the amorphous layer covering the Se nanowires. The oxide layer may form during the growth, and the oxygen may come from the adsorbed oxygen of the source powders, the system leakage, and the residual oxygen gas. Therefore, we can conclude that our samples consist of Se and they are well crystallized and sheathed by a thin layer of amorphous oxide materials.

Raman scattering has proven to be a versatile technique to characterize nanostructured materials.¹¹ To further investigate the crystal quality of as-prepared Se nanowires, we measured the Raman spectrum of the as-prepared Se nanowires along with that of Se powder for comparison, as shown in Figure 3b. An intensive peak at 237.3 cm^{-1} is observed in the Raman spectra of Se powder, which is attributed to the Raman scattering of the A_1 mode of hexagonal selenium.² Moreover, two 2nd-order modes at about 440 and 458 cm^{-1} are also observed. They correspond to the combination mode and overtone of the phonons at the edge point (M) of the Brillouin zone.¹² The Raman spectrum of as-prepared Se nanowires shows a spectral feature similar to that of Se powder. The peak frequency (237.3 cm^{-1}) and narrow half-width at maximum (9.0 cm^{-1}) of the A_1 mode in Se nanowires indicate that the as-prepared Se nanowires have a high crystal quality, and because the diameter of Se nanowires is large enough, the quantum confinement effect on the peak frequency can be ignored. Furthermore, no

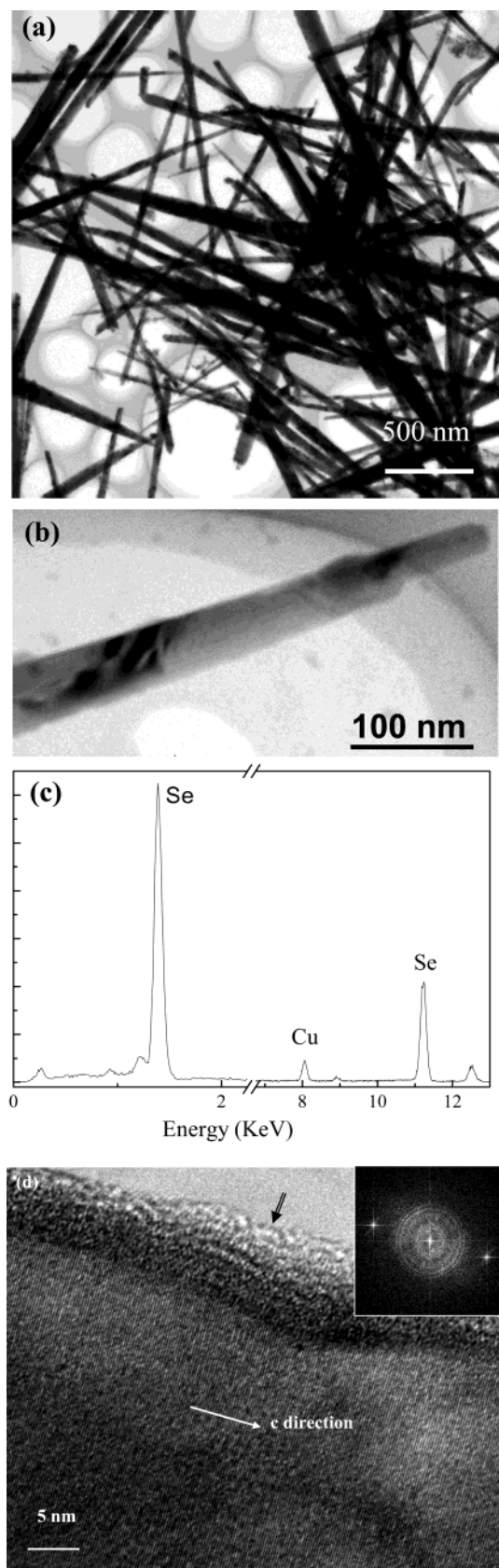


Figure 2. (a) TEM image of the Se nanowires. The diameters of the Se nanowires vary in the range between 20 and 300 nm. (b) Magnified TEM image of a single Se nanowire. (c) The corresponding EDS spectrum of the single Se nanowire. Only Se is detected, confirming the nanowires are composed of selenium, while the C and Cu peaks come from the holey carbon film grids. (d) HRTEM image showing the microstructure details of a single Se nanowire. The wire axis is found parallel to the *c*-axis direction of the hexagonal Se crystal.

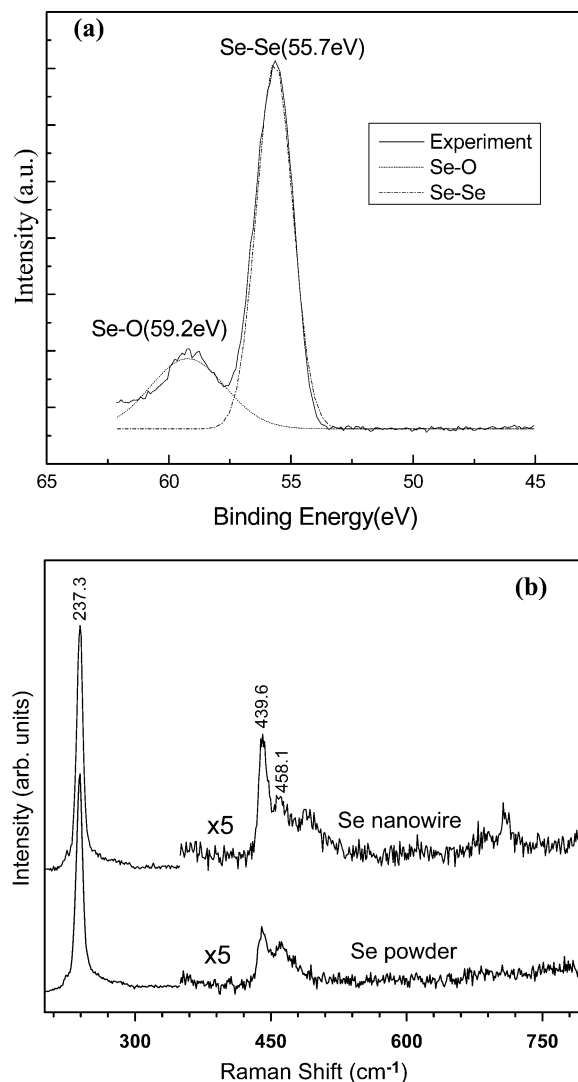


Figure 3. (a) XPS spectrum of the Se nanowires. It is visible that Se–Se bonds dominate in the products, and a small portion of Se–O bonds was also revealed. (b) Raman spectrum of the Se nanowires in comparison with that of the bulk Se powder.

observation of any signals of the 256-cm^{-1} peak for monoclinic selenium and of the 264-cm^{-1} peak for amorphous selenium³ indicates that almost no monoclinic selenium or amorphous selenium is contained in the prepared samples. Although the Se nanowires are covered with an amorphous oxide layer of a thickness about 2 nm, they appear to be weak in the Raman spectra because of small amount of amorphous Se oxide in the prepared samples.

A series of experiments were done to explore the growth mechanism of the Se nanowires. Different catalysts such as Cu, Fe, Ni, and Si were added into the source materials, and we find that only silicon is effective in the growth of the Se nanowires. In fact, only large sphere-shaped bubbles were formed if no Si was used (Figure 1c). Therefore, a preliminary model was proposed to explain the growth of the Se nanowires, in particular, the role that the Si may play in the growth of the Se nanowires. There exists a reaction during the growth:



Silicon and selenium can react to form SiSe_2 , which will decrease the concentration of Se vapor and as a result prevent the formation of large Se bubbles, which is in favor of the

nanowire growth. The SiSe₂ is solid and remained at the site of the Si source. That can explain how the Si was involved in the growth of the Se nanowires, and why the SiSe₂ compound was not observed in the final nanowires. The SiSe₂ is highly sensitive to H₂O and forms volatile H₂Se, which was indicated by the particular odor of H₂Se when opening the reaction tube. This reaction prevents us from further identifying SiSe₂ by other means such as XRD. Because the use of Si is solely to reduce the Se vapor pressure, however, a question arises: is it possible to grow selenium nanowires by simply reducing the sublimation temperature of selenium? We believe it may be possible with finely adjusted parameters of growth such as pressure, gas flow, and temperatures. For the present case, our experimental results indicate the necessity of using Si. An appropriate temperature gradient was required for the nucleation of the Se nanowires. It means we have to elevate the temperature of the reactant to at least 680 °C. As discussed in the above, using Si is the effective way to reduce the Se vapor pressure at such high temperature.

The growth temperature has a significant effect on the diameters of the nanowires, and the mean diameter of the Se nanowires increased as the temperature increased. Systematic work has revealed that the mean diameters of the nanowires grown at 750 °C, 850 °C, and 950 °C were statistically around 75, 83, and 90 nm, respectively. This is typical for vapor-phase homogeneous nucleation. According to the basic thermodynamics, the sizes of the critical nuclei are given by Gibbs-Thompson's formula:

$$r_c = \frac{\nu\sigma}{kT \ln \frac{P}{P_s}} \quad (2)$$

where P_s is the saturation pressure of the vapor, P is the pressure of the reaction site, σ is the surface specific energy of the nucleus, ν is the molecular volume, and T is the temperature. From this equation, it is evident that the critical radius of a nucleus r_c decreases as the temperature increases. The homogeneous nucleation rate can be written as

$$\dot{N} = 4\pi r_c^2 \Phi n_s \exp\left(-\frac{\Delta G^*}{kT}\right) \quad (3)$$

where Φ is the atom impingement flux, n_s is the density of all possible nucleation sites, and ΔG^* is the energy barrier to the nucleation process. Equations 2 and 3 indicate that the solid phase is easier to form at a higher temperature and the number of the nuclei is larger than that at low temperature. Hence, the coalescence of the nuclei is dominated so that the burgeoning nuclei can accumulate to form a larger growth seed and the mean diameters become larger at high temperature, which is in good agreement with our experimental results. There are two vital factors for the one-dimensional growth of the Se nanowires. One is the steep temperature gradient, which provides an extrinsic driving force for the growth. The other is the peculiar

crystal structure of the Se, which is the intrinsic reason for the preferable 1-D growth. Because the hexagonal Se is asymmetric and exhibits a chain-structure along the (001) c -axis direction, it has a much faster growth along the c -axis direction,³ as is revealed in the HRTEM image in Figure 2d. The above-discussed model can explain some of the experimental results; however, the real growth mechanism of the Se nanowires still remains a problem for further investigation.

Conclusions

Se nanowires were synthesized through a simple physical evaporation by using Si as an assistant source material. XRD patterns of the samples demonstrate that the nanowires have a pure hexagonal Se phase. EDS and XPS results confirmed that the nanowires consist of Se, while a small amount of Se is in the state of Se–O bonds sheathing the nanowires. TEM and SEM revealed that the length of nanowires is up to several micrometers and the diameter of nanowires can be as thin as 20 nm. HRTEM analysis depicted the detailed crystalline structures of the Se nanowires. Raman spectra of Se nanowires were compared with that of the bulk Se powder.

Acknowledgment. This project was financially supported by the National Natural Science Foundation of China (NSFC, No. 50025206, 20151002), the Scientific Research Foundation for the Returned Overseas Chinese Scholars, State Education Ministry, and national 973 projects (No. 2002CB613505, MOST, P. R. China). D. P. Yu is obliged to the financial support from Cheung Kong Scholar program, and L. Ren is grateful to the Chun-Tsung Fund, Peking University, for the program of the research experiences for undergraduates.

References and Notes

- (1) Muth, O. H.; Oldfield, J. E.; Weswig, P. H. *Symposium: Selenium in Biomedicine*, 7–26.
- (2) Cooper, W. C. *The physics of selenium and tellurium*; 3–20.
- (3) Gates, B.; Mayers, B.; Cattle, B.; Xia, Y. N. *Adv. Funct. Mater.* **2002**, *12*, 219–227.
- (4) Ibragimov, N. I.; Abutalibova, Z. M.; Agaev, V. G. *Thin Solid Films* **2000**, *359*, 125–126.
- (5) (a) Morales, M.; Lieber, C. M. *Science* **1998**, *279*, 208–211, (b) Yu, D. P.; Lee, C. S.; Bello, I.; Sun, X. S.; Zhou, G. W.; Bai, Z. G.; Zhang, Z.; Feng, S. Q. *Solid State Commun.* **1998**, *105*, 403–407. (c) Mayers, B.; Gates, B.; Yin, Y. D.; Xia, Y. N. *Adv. Mater.* **2001**, *13*, 1380–1384.
- (6) (a) Yu, D. P.; Bai, Z. G.; Wang, J. J.; Zou, Y. H.; Qian, W.; Zhang, H. Z.; Ding, Y.; Xiong, G. C.; Feng, S. Q. *Phys. Rev. B* **1999**, *59*, R2498–R2501. (b) Yu, D. P.; Bai, Z. G.; Ding, Y.; Hang, Q. L.; Zhang, H. Z. *Appl. Phys. Lett.* **1998**, *72*, 3458–3460. (c) Prokes, S. M.; Wang, K. L. *MRS Bull.* **1999**, *24*, 13–19.
- (7) Jiang, Z. Y.; Xie, Z. X.; Xie, S. Y.; Zhang, X. H.; Huang, R. B.; Zheng, L. S. *Chem. Phys. Lett.* **2003**, *368*, 425–429.
- (8) Lickes, J. P.; Dumont, F. C.; Buess-Herman, C. *Colloids Surf. A* **1996**, *118*, 167–170.
- (9) Abdelouas, A.; Gong, W. L.; Lutze, W.; Shelnut, J. A.; Franco, R.; Moura, I. *Chem. Mater.* **2000**, *12*, 1510–1512.
- (10) Zhang, H. Z.; Yu, D. P.; Ding, Y.; Bai, Z. G.; Hang, Q. L.; Feng, S. Q. *Appl. Phys. Lett.* **1998**, *73*, 3396–3398.
- (11) Tan, P. H.; Brunner, K.; Bougeard, D.; Abstreiter, G. *Phys. Rev. B*, in press.
- (12) Martin, R. M.; Lucovsky, G.; Helliwell, K. *Phys. Rev. B* **1976**, *13*, 1383–1395.